

Effect of fast harmonic excitation on frequency-locking in a van der Pol–Mathieu–Duffing oscillator

Abdelhak Fahsi ^a, Mohamed Belhaq ^{b,*}

^a *Department of Mathematics, FSTM, University Hassan II-Mohammadia, Morocco*

^b *Laboratory of Mechanics, University Hassan II-Aïn Chock, Casablanca, Morocco*

Received 3 May 2007; received in revised form 10 July 2007; accepted 16 July 2007

Available online 31 July 2007

Abstract

We study the effect of high-frequency harmonic excitation on the entrainment area of the main resonance in a van der Pol–Mathieu–Duffing oscillator. An averaging technique is used to derive a self- and parametrically driven equation governing the slow dynamic of the oscillator. The multiple scales method is then performed on the slow dynamic near the main resonance to obtain a reduced autonomous slow flow equations governing the modulation of amplitude and phase of the slow dynamic. These equations are used to determine the steady state response, bifurcation and frequency–response curves. A second multiple scales expansion is used for each of the dependent variables of the slow flow to obtain *slow slow* flow modulation equations. Analysis of non-trivial equilibrium of this *slow slow* flow provides approximation of the slow flow limit cycle corresponding to quasi-periodic motion of the slow dynamic of the original system. Results show that fast harmonic excitation can change the nonlinear characteristic spring behavior and affect significantly the entrainment region. Numerical simulations are used to confirm the analytical results.

© 2007 Elsevier B.V. All rights reserved.

PACS: 02.30.Hq; 02.30.Oz; 02.30.Mv; 46.40.Ff

Keywords: Fast excitation; Self-excitation; Parametric forcing; Frequency-locking

1. Introduction

In this paper, we study the influence of adding fast harmonic (FH) excitation on the entrainment area of the main parametric resonance for a self- and parametrically (SP) excited oscillator of van der Pol–Mathieu–Duffing type. Entrainment or frequency-locking phenomenon in self-excited systems subjected to harmonic excitation occurs in various mechanical systems. It can take place when a limit cycle is entrained by the main resonance causing the system to vibrate at the resonance frequency with a relatively large amplitude of motion. This phenomenon was considered by many authors. Tondl [1] investigated SP excited oscillators with one and two degrees of freedom and provided entrainment areas. Schmidt [2] analyzed interaction of SP excited

* Corresponding author.

E-mail address: mbelhaq@yahoo.fr (M. Belhaq).

vibrations. Szabelski and co-workers [3,4] examined the interaction between parametric, nonparametric and self-excited vibrations in systems with one or two degrees of freedom. Belhaq et al. [5] and Belhaq [6] studied SP excited oscillator near the 4:1 resonance and determined the entrained oscillations and the quasi-periodic zone. Similar results near 1:1, 2:1 and 3:1 resonances were also analyzed in [7]. Yano [8,9] considered vibrations of SP excited systems and determined amplitude modulation of the quasi-periodical vibrations and synchronized motion while Abouhazim et al. [10] investigated entrainment near the 2:2:1 resonance in an SP quasi-periodic Mathieu oscillator. Recently, Pandey et al. [11] studied frequency-locking in a forced Mathieu–van der Pol–Duffing system and provided application in optically driven MEMS resonators [12].

Furthermore, the study of non-trivial effects of FH excitation on the slow dynamic of mechanical systems has been considered in recent years [13,14]. A such excitation can affect certain characteristics of systems such as equilibrium stability [15], linear stiffness [16], damping [17], natural frequencies [18], stik-slip dynamics [19], symmetry breaking [20] and Hopf bifurcation [21,22]. To analyze these non-trivial effects, the method of direct partition of motion (DPM) [23] is usually used to reduce the FH excited oscillator into an autonomous equation governing the averaged slow dynamic.

The present paper deals with the effect of FH excitation on a van der Pol–Mathieu–Duffing oscillator. We focus an attention on the influence of FH excitation on the frequency-locking area of the main resonance. We use the method of DPM to derive an SP excited equation governing the slow dynamic of the oscillator. The multiple scales method is then applied on the slow dynamic to derive an autonomous slow flow in the neighborhood of the 2:1 resonance. Analysis of equilibrium points of this slow flow provides analytical approximations of the amplitude of the entrained response. The limit cycle is investigated by constructing analytical expressions of the periodic solution of the slow flow. We perform numerical study and we compare the obtained results to the analytical finding for validation.

2. Slow motion

Consider the following van der Pol–Mathieu–Duffing oscillator subjected to an FH excitation

$$\ddot{x} + (1 - h \cos \omega t)x - (\alpha - \beta x^2)\dot{x} - \gamma x^3 = a\Omega^2 \cos x \cos \Omega t \tag{1}$$

where damping α , β , nonlinearity γ and excitation amplitudes h and a are small. Dots denote differentiation with respect to time t . We assume that the frequency Ω is large compared to ω such that resonance phenomena with the frequency Ω are avoided.

To analyze the influence of high-frequency excitation on the slow dynamic of system (1), it is convenient to use the method of DPM [23]. To implement the method, we introduce two different time scales: a fast time $T_0 = \Omega t$ and a slow time $T_1 = t$. Next, we split up $x(t)$ into a slow part $z(T_1)$ and a fast part $\epsilon\phi(T_0, T_1)$ as follows:

$$x(t) = z(T_1) + \epsilon\phi(T_0, T_1) \tag{2}$$

where z describes slow main motions at time-scale of oscillations, $\epsilon\phi$ stands for an overlay of the fast motions and ϵ indicates that $\epsilon\phi$ is small compared to z . Since Ω is considered as a large parameter we choose $\epsilon \equiv \Omega^{-1}$, for convenience. The fast part $\epsilon\phi$ and its derivatives are assumed to be 2π -periodic functions of fast time T_0 with zero mean value with respect to this time, so that $\langle x(t) \rangle = z(T_1)$, where $\langle \cdot \rangle \equiv \frac{1}{2\pi} \int_0^{2\pi} (\cdot) dT_0$ defines time-averaging operator over one period of the fast excitation with the slow time T_1 fixed.

Introducing $D_i^j \equiv \frac{\partial^j}{\partial T_i^j}$ yields $\frac{d}{dt} = \Omega D_0 + D_1$, $\frac{d^2}{dt^2} = \Omega^2 D_0^2 + 2\Omega D_0 D_1 + D_1^2$ and substituting (2) into (1) gives

$$\begin{aligned} \epsilon^{-1} D_0^2 \phi + 2D_0 D_1 \phi + \epsilon D_1^2 \phi + D_1^2 z + (1 - h \cos \omega T_1)(z + \epsilon\phi) - (\alpha - \beta(z + \epsilon\phi)^2)(D_0 \phi + \epsilon D_1 \phi + D_1 z) - \gamma(z + \epsilon\phi)^3 \\ = \epsilon^{-1} (a\Omega) \cos(z + \epsilon\phi) \cos T_0. \end{aligned} \tag{3}$$

Averaging (3) leads to

$$D_1^2 z + (1 - h \cos \omega T_1)z - (\alpha - \beta z^2)D_1 z - \gamma z^3 = \epsilon^{-1} (a\Omega) \langle \cos(z + \epsilon\phi) \cos T_0 \rangle. \tag{4}$$

Subtracting (4) from (3) yields

$$\begin{aligned} \epsilon^{-1} D_0^2 \phi + 2D_0 D_1 \phi + \epsilon D_1^2 \phi + (1 - h \cos \omega T_1)\epsilon\phi - (\alpha - \beta z^2)(D_0 \phi + \epsilon D_1 \phi) + \beta(2\epsilon\phi + \epsilon^2 \phi^2)(D_0 \phi + \epsilon D_1 \phi) \\ - \gamma(3\epsilon z^2 \phi + 3\epsilon^2 z \phi^2 + \epsilon^3 \phi^3) \\ = \epsilon^{-1} (a\Omega) \cos(z + \epsilon\phi) \cos T_0 - \epsilon^{-1} (a\Omega) \langle \cos(z + \epsilon\phi) \cos T_0 \rangle. \end{aligned} \tag{5}$$

An approximate expression for $\epsilon\phi$ is obtained from (5) by considering only the dominant terms of order ϵ^{-1} as

$$D_0^2\phi = (a\Omega) \cos z \cos T_0 \quad (6)$$

where it is assumed that $a\Omega = O(\epsilon^0)$. The stationary solution to the first order for ϕ is written as

$$\epsilon\phi = -a \cos z \cos T_0. \quad (7)$$

The equation governing the slow motion is derived from (4). Inserting $\cos(z + \epsilon\phi) = \cos z - \epsilon\phi \sin z + O(\epsilon^2)$ into Eq. (4) and retaining the dominant terms of order ϵ^0 , we obtain

$$D_1^2z + (1 - h \cos \omega T_1)z - (\alpha - \beta z^2)D_1z - \gamma z^3 = -(a\Omega) \sin z \langle \phi \cos T_0 \rangle. \quad (8)$$

Inserting ϕ from (7) and using that $\langle \cos^2 T_0 \rangle = 1/2$ we find the approximate equation for slow motions

$$D_1^2z + (1 - h \cos \omega T_1)z - (\alpha - \beta z^2)D_1z - \gamma z^3 = \frac{1}{2}(a\Omega)^2 \cos z \sin z \quad (9)$$

which is similar to the original equation (1) in which the non-autonomous term $a\Omega^2 \cos x \cos \Omega t$ is replaced by the autonomous one $\frac{1}{2}(a\Omega)^2 \cos z \sin z$. We focus the analysis on small vibrations around the origin by expanding in Taylor's series the terms $\sin z \simeq z - z^3/6$ and $\cos z \simeq 1 - z^2/2$. Keeping only terms up to order three in z , Eq. (9) becomes

$$D_1^2z + (1 - \frac{1}{2}(a\Omega)^2 - h \cos \omega T_1)z - (\alpha - \beta z^2)D_1z - (\gamma - \frac{1}{3}(a\Omega)^2)z^3 = 0. \quad (10)$$

Note that in Eq. (10) the influence of frequency Ω is introduced in the natural frequency of the system and in the nonlinear stiffness coefficient.

3. Slow flow and entrainment

We rewrite Eq. (10) in the following form

$$\ddot{z} + \omega_0^2 z = (\alpha - \beta z^2)\dot{z} + \xi z^3 + hz \cos \omega t \quad (11)$$

where $\omega_0^2 = 1 - \frac{1}{2}(a\Omega)^2$ and $\xi = \gamma - \frac{1}{3}(a\Omega)^2$. We express the main resonant condition by introducing a detuning parameter σ according to

$$\omega_0^2 = \frac{\omega^2}{4} + \sigma. \quad (12)$$

We apply a double perturbation technique [24,25] by introducing two small bookkeeping parameters μ and η . To implement the first perturbation we use the parameter μ and for the second step perturbation we introduce the other parameter η . Hence, Eq. (11) is rewritten as

$$\ddot{z} + \frac{\omega^2}{4} z = \mu \{ -\sigma z + (\alpha - \beta z^2)\dot{z} + \xi z^3 + hz \cos \omega t \}. \quad (13)$$

Using the multiple scales technique [27], we seek a solution to Eq. (13) in the form

$$z(t) = z_0(T_1, T_2) + \mu z_1(T_1, T_2) + O(\mu^2) \quad (14)$$

where $T_1 = t$ and $T_2 = \mu t$. In terms of the variables T_i , the time derivatives become $\frac{d}{dt} = D_1 + \mu D_2 + O(\mu^2)$ and $\frac{d^2}{dt^2} = D_1^2 + 2\mu D_1 D_2 + O(\mu^2)$ where $D_i^j = \frac{\partial^j}{\partial T_i^j}$. Substituting Eq. (14) into Eq. (13) and equating coefficients of like powers of μ , we obtain

– Order μ^0 :

$$D_1^2 z_0 + \frac{\omega^2}{4} z_0 = 0. \quad (15)$$

– Order μ^1 :

$$D_1^2 z_1 + \frac{\omega^2}{4} z_1 = -2D_1 D_2 z_0 - \sigma z_0 + (\alpha - \beta z_0^2) D_1 z_0 + \zeta z_0^3 + h z_0 \cos \omega T_1. \tag{16}$$

The solution to the first order is given by

$$z_0(T_1, T_2) = r(T_2) \cos\left(\frac{\omega}{2} T_1 + \theta(T_2)\right). \tag{17}$$

Substituting Eq. (17) into Eq. (16) and removing secular terms, we obtain the slow flow modulation equations of amplitude and phase

$$\begin{aligned} \frac{dr}{dT_2} &= \frac{\alpha}{2} r - \frac{\beta}{8} r^3 - \frac{h}{2\omega} r \sin(2\theta) \\ \frac{d\theta}{dT_2} &= \frac{\sigma}{\omega} - \frac{3\zeta}{4\omega} r^2 - \frac{h}{2\omega} \cos(2\theta). \end{aligned} \tag{18}$$

Note that the system (18) is invariant under the transformation $\theta \rightarrow -\theta + \frac{\pi}{2}$, $\sigma \rightarrow -\sigma$ and $\zeta \rightarrow -\zeta$. This allows one to replace in Eq. (18) σ by $s\sigma$ and ζ by $s\zeta$ with $s = \pm 1$. Thus system (18) reads

$$\begin{aligned} \frac{dr}{dT_2} &= \frac{\alpha}{2} r - \frac{\beta}{8} r^3 - \frac{h}{2\omega} r \sin(2\theta) \\ \frac{d\theta}{dT_2} &= \frac{s\sigma}{\omega} - \frac{3s\zeta}{4\omega} r^2 - \frac{h}{2\omega} \cos(2\theta). \end{aligned} \tag{19}$$

Equilibrium points of the slow flow (19), corresponding to periodic oscillations of Eq. (11), are determined by setting $\frac{dr}{dT_2} = \frac{d\theta}{dT_2} = 0$. Using the trig identity $\cos^2\theta + \sin^2\theta = 1$ and we define $\rho = r^2$, we obtain the following quadratic equation in ρ

$$\left(\frac{\beta^2}{64} + \frac{9\zeta^2}{16\omega^2}\right)\rho^2 - \left(\frac{\alpha\beta}{8} + \frac{3\sigma\zeta}{2\omega^2}\right)\rho + \frac{\alpha^2}{4} + \frac{\sigma^2}{\omega^2} - \frac{h^2}{4\omega^2} = 0. \tag{20}$$

Eq. (20) has two real roots if the discriminant Δ is nonnegative. This gives the condition

$$\Delta = \left(\frac{\alpha\beta}{16} + \frac{3\sigma\zeta}{4\omega^2}\right)^2 - \left(\frac{\beta^2}{64} + \frac{9\zeta^2}{16\omega^2}\right)\left(\frac{\alpha^2}{4} + \frac{\sigma^2}{\omega^2} - \frac{h^2}{4\omega^2}\right) > 0. \tag{21}$$

These two solutions are positive if the two following conditions are held

$$C = \frac{\alpha^2}{4} + \frac{\sigma^2}{\omega^2} - \frac{h^2}{4\omega^2} > 0, \quad B = \frac{\alpha\beta}{4} + \frac{3\sigma\zeta}{\omega^2} > 0. \tag{22}$$

Furthermore, Eq. (20) has only one positive root if the following condition is satisfied

$$C < 0. \tag{23}$$

In what follows we fix the parameters $\alpha = 0.01$, $\beta = 0.05$, $\gamma = 0.1$, $h = 0.1$, and $a = 0.02$.

In Fig. 1a the frequency response curve, as given by Eq. (20), is presented for $\Omega = 0$ exhibiting stable entrainment oscillations. The effect of the excitation frequency Ω on the frequency-locking area is illustrated in Fig. 1b–d for the values $\Omega = 25$, $\Omega = 40$ and $\Omega = 50$, respectively. It can be seen that as the frequency Ω increases, the entrainment area shifts left and the nonlinear characteristic stiffness changes causing the system to switch from softening to hardening behavior. Analytical approximations (solid line for stable oscillations and dashed line for unstable ones) are compared to numerical integration (circles) using a Runge–Kutta method.

Fig. 2a illustrates the bifurcation curves of periodic solutions of the slow dynamic (11) for $\Omega = 0$. We can distinct three regions. In region I, where conditions (21) and (23) are satisfied, there are two possible solutions: an unstable trivial solution and a larger stable one. Within region II, where conditions (21) and (22) are satisfied, there are three possible solutions: one unstable, one larger stable and the trivial unstable solution. Within the regions III and IV only an unstable trivial solution exists. In these regions a limit cycle exists and it is stable. Fig. 2b is plotted for $\Omega = 40$ showing the effect of Ω on the bifurcation curves. It can be seen that, as Ω increases, region I switches from the right branch of the curve $\Delta = 0$ to the left one causing an

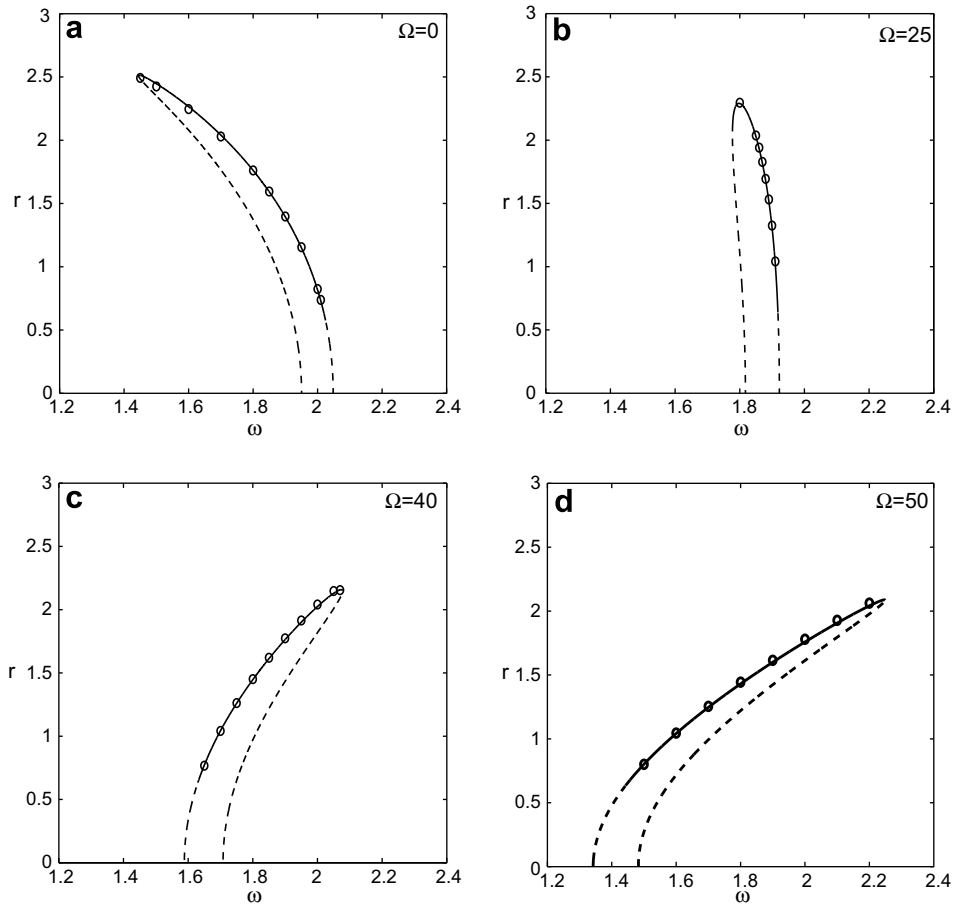


Fig. 1. Amplitude frequency response near 2:1 resonance. Analytical approximation: Solid (for stable) and dashed for (unstable). Numerical simulation: circles.

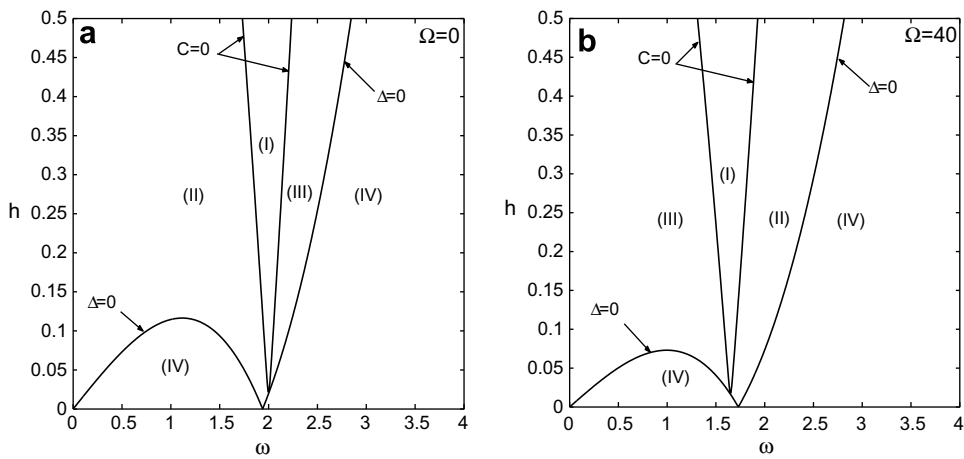


Fig. 2. Bifurcation curves of periodic solutions of the slow dynamic (11) near 2:1 resonance.

exchange between regions II and III inside the curve $\Delta = 0$. This behavior is consistent with the spring characteristic change of the backbone curve in Fig. 1.

4. Slow flow and limit cycle

In this section we construct analytical approximation of the limit cycle of the slow flow (19) corresponding to quasi-periodic motion of the slow dynamic (11).

We transform the polar form (19) using the variable change

$$u = r \cos \theta, \quad v = -r \sin \theta \tag{24}$$

to the cartesian system

$$\begin{aligned} \frac{du}{dT_2} &= \left(\frac{s\sigma}{\omega} + \frac{h}{2\omega}\right)v + \eta \left\{ \frac{\alpha}{2}u - \left(\frac{\beta}{8}u + \frac{3s\xi}{4\omega}v\right)(u^2 + v^2) \right\} \\ \frac{dv}{dT_2} &= -\left(\frac{s\sigma}{\omega} - \frac{h}{2\omega}\right)u + \eta \left\{ \frac{\alpha}{2}v - \left(\frac{\beta}{8}v - \frac{3s\xi}{4\omega}u\right)(u^2 + v^2) \right\}. \end{aligned} \tag{25}$$

To implement the second perturbation step, η is introduced in the damping and nonlinearity.

Following [24,25], we approximate periodic solution of the slow flow (25) by using a multiple scales perturbation expansion. We expand

$$\begin{aligned} u(T_2, T_3) &= u_0(T_2, T_3) + \eta u_1(T_2, T_3) + O(\eta^2) \\ v(T_2, T_3) &= v_0(T_2, T_3) + \eta v_1(T_2, T_3) + O(\eta^2) \end{aligned} \tag{26}$$

where $T_2 = \mu t$ and $T_3 = \eta T_2 = \eta \mu t$. Introducing $D_i = \frac{\partial}{\partial T_i}$ yields $\frac{d}{dT_2} = D_2 + \eta D_3 + O(\eta^2)$. Substituting Eqs. (26) into Eqs. (25) and collecting terms, we get

– Order η^0 :

$$\begin{aligned} D_2^2 u_0 + v^2 u_0 &= 0, \\ \left(\frac{s\sigma}{\omega} + \frac{h}{2\omega}\right)v_0 &= D_2 u_0 \end{aligned} \tag{27}$$

– Order η^1 :

$$\begin{aligned} D_2^2 u_1 + v^2 u_1 &= \left(\frac{s\sigma}{\omega} + \frac{h}{2\omega}\right) \left[-D_3 v_0 + \frac{\alpha}{2}v_0 - \left(\frac{\beta}{8}v_0 - \frac{3s\xi}{4\omega}u_0\right)(u_0^2 + v_0^2) \right] \\ &\quad - D_2 D_3 u_0 + \frac{\alpha}{2}D_2 u_0 - D_2 \left[\left(\frac{\beta}{8}u_0 + \frac{3s\xi}{4\omega}v_0\right)(u_0^2 + v_0^2) \right], \\ \left(\frac{s\sigma}{\omega} + \frac{h}{2\omega}\right)v_1 &= D_2 u_1 + D_3 u_0 - \frac{\alpha}{2}u_0 + \left(\frac{\beta}{8}u_0 + \frac{3s\xi}{4\omega}v_0\right)(u_0^2 + v_0^2) \end{aligned} \tag{28}$$

where $\nu = \sqrt{\left(\frac{\alpha}{\omega}\right)^2 - \left(\frac{h}{2\omega}\right)^2}$ is the proper frequency of system (25) corresponding to the frequency of the slow flow limit cycle.

The solution to the first order system (27) is given by

$$\begin{aligned} u_0(T_2, T_3) &= R(T_3) \cos(\nu T_2 + \varphi(T_3)) \\ v_0(T_2, T_3) &= -\frac{\nu}{\left(\frac{s\sigma}{\omega} + \frac{h}{2\omega}\right)} R(T_3) \sin(\nu T_2 + \varphi(T_3)). \end{aligned} \tag{29}$$

Here $R(T_3)$ and $\varphi(T_3)$ are functions of $T_3 = \eta T_2$. Since $T_2 = \mu t$ is slow time, and since we have assumed η to be small, we shall refer to T_3 as “slow slow time” or “s.s. time” for breveting [26].

Substituting (29) into (28) and removing secular terms gives the following autonomous s.s. flow system on R and φ

$$\begin{aligned} \frac{dR}{dT_3} &= \frac{\alpha}{2}R - \frac{s\beta\sigma}{8s\sigma + 4h}R^3, \\ \frac{d\varphi}{dT_3} &= -\frac{3s\xi(8\sigma^2 + h^2)}{8\omega(2s\sigma + h)\sqrt{4\sigma^2 - h^2}}R^2 \end{aligned} \tag{30}$$

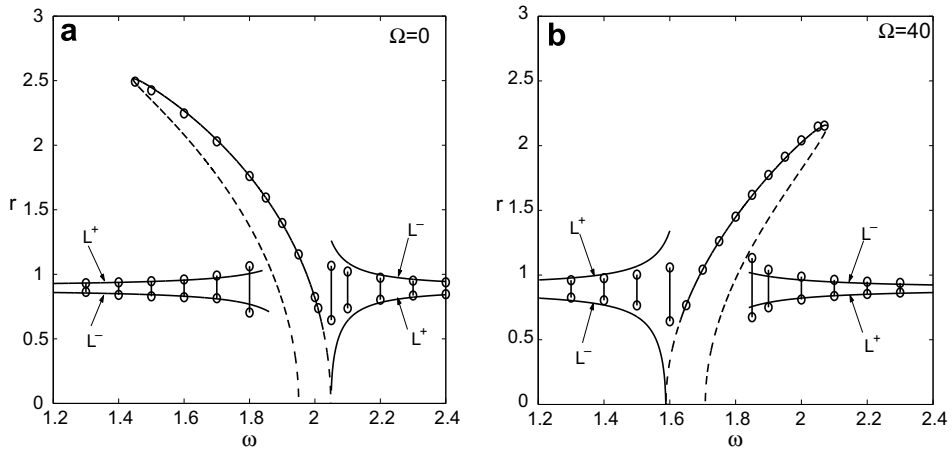


Fig. 3. Effect of the frequency Ω on the entrainment area and on the modulation amplitude vibration.

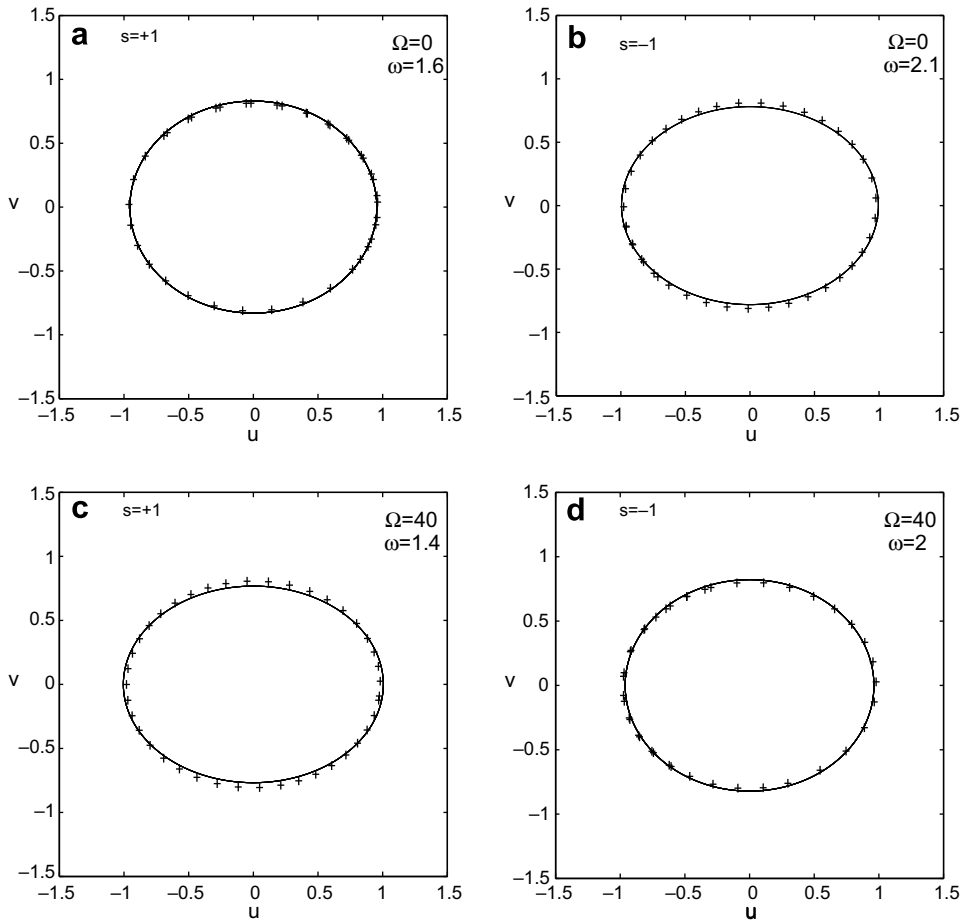


Fig. 4. Comparisons between analytical approximation (solid line) of periodic solution, Eq. (32), and numerical integration (plus signs) of the slow flow (25).

Equilibria in Eqs. (30) are obtained by setting $\frac{dR}{dT_3} = 0$ and given by

$$R = 0, \quad R = \sqrt{\frac{2\alpha(2s\sigma + h)}{s\beta\sigma}}. \tag{31}$$

The non-trivial equilibrium in Eq. (31) will correspond to the amplitude of the limit cycle of the slow flow (25) and to quasi-periodic oscillations in the slow dynamic (11). In Fig. 3a and b we draw for the two different values $\Omega = 0$ and $\Omega = 40$ the analytical amplitude of the slow flow limit cycle, Eq. (31), and the entrainment area as given by Eq. (20). The curves labelled L^+ correspond to $s = +1$ in Eq. (31) and the curves labelled L^- correspond to $s = -1$. The shift of the entrainment area can be clearly seen. The numerical modulation amplitude vibrations (quasi-periodic oscillations) are marked with double circles connected with a vertical line. Comparison of analytical results and numerical integration of the modulation amplitude motion shows a good agreement.

The approximate periodic solution to system (25) is given by

$$\begin{aligned} u(T_2) &= R \cos(vT_2 + \varphi) \\ v(T_2) &= -\frac{2v\omega}{(2s\sigma + h)} R \sin(vT_2 + \varphi) \end{aligned} \tag{32}$$

where

$$\varphi = -\frac{3s\xi(8\sigma^2 + h^2)}{8\omega(2s\sigma + h)\sqrt{4\sigma^2 - h^2}} R^2 T_3 \tag{33}$$

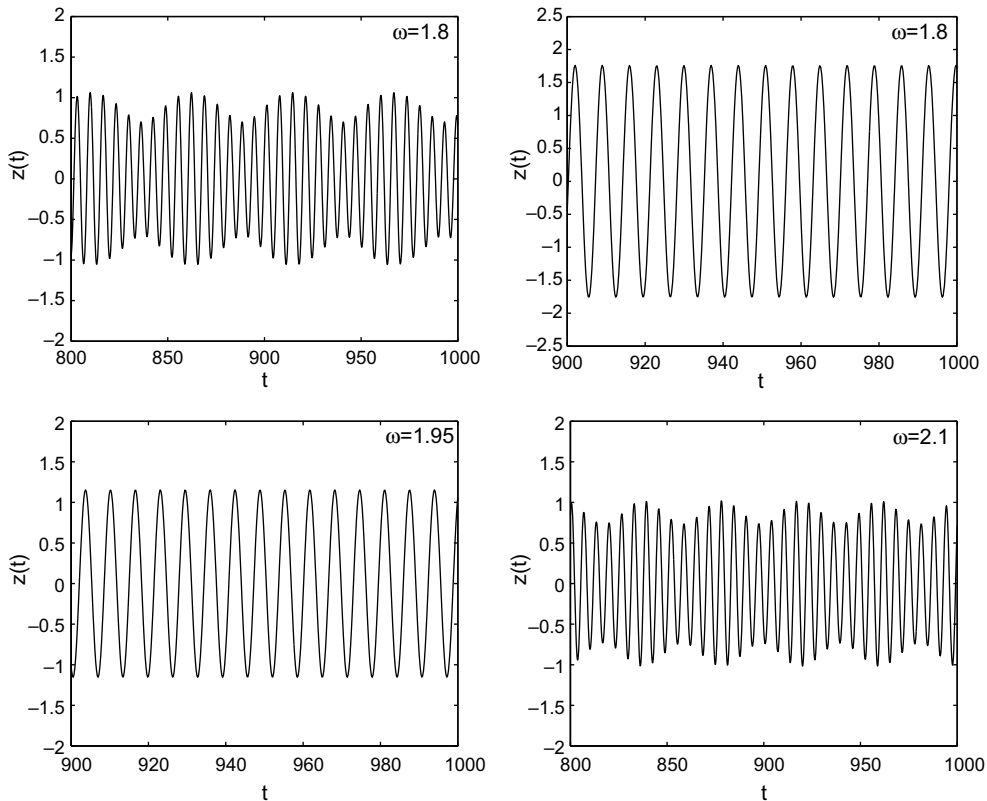


Fig. 5. Examples of time histories of the slow dynamic $z(t)$ by numerical integration for $\Omega = 0$.

and the quasi-periodic oscillation of the slow dynamic system (11) is written as

$$z(t) = u(T_2) \cos\left(\frac{\omega}{2}t\right) + v(T_2) \sin\left(\frac{\omega}{2}t\right). \quad (34)$$

To validate the analytical finding, we show in Fig. 4 comparisons between the approximate periodic solution (32) and the numerical integration of the slow flow (25) using Runge–Kutta method. Fig. 4a and c are plotted for $s = +1$ and Fig. 4b and d are plotted for $s = -1$.

In Fig. 5 we present examples of time histories of the slow dynamic $z(t)$ obtained by numerical simulations.

5. Conclusion

The influence of FH parametric excitation on the frequency-locking area to the principal parametric resonance in a van der Pol–Mathieu–Duffing oscillator has been studied analytically and numerically. The use of the DPM technique followed by two successive multiple scales methods reduces successively the original oscillator to a slow dynamic, a slow flow and an s.s. flow. The analysis of equilibria of slow flow and s.s. flow provides information on periodic and quasi-periodic oscillations of the slow motion, respectively. Results show that FH excitation can change the nonlinear characteristic spring behavior of the system from softening to hardening and causes the entrainment area to shift. In contrast, no significant effect on the amplitudes of both entrained and quasi-periodic responses is noticed. It was also shown that controlling and adjusting the entrainment area to a desired frequency range near a resonance may be achieved by acting only on the frequency Ω . This can be of interest from engineering applications point of view.

References

- [1] Tondl A. On the interaction between self-excited and parametric vibrations. National Research Institute for Machine Design, Monographs and Memoranda No. 25, Prague; 1978.
- [2] Schmidt G. Interaction of self-excited forced and parametrically excited vibrations. The 9th international conference on nonlinear oscillations. Application of the theory of nonlinear oscillations, vol. 3. Kiev: Naukova Dumka; 1984.
- [3] Szabelski K, Warminski J. Self-excited system vibrations with parametric and external excitations. *J Sound Vib* 1995;187(4):595–607.
- [4] Szabelski K, Warminski J. The nonlinear vibrations of parametrically self-excited system with two degrees of freedom under external excitation. *Nonlinear Dynam* 1997;14:23–36.
- [5] Belhaq M, Clerc RL, Hartman C. Etude numérique d'une 4-résonance d'une équation de Liénard forcée. *CR Acad Sci Paris* 1986;303(II-10):873–6.
- [6] Belhaq M. Numerical study for parametric excitation of differential equation near a 4-resonance. *Mech Res Commun* 1990;17(4):199–206.
- [7] Belhaq M, Fahsi A. Higher-order approximation of subharmonics close to strong resonances in the forced oscillators. *Comput Math Appl* 1997;33(8):133–44.
- [8] Yano S. Analytic research on dynamic phenomena of parametrically and self-excited mechanical systems. *Ing Arch* 1987;57:51–60.
- [9] Yano S. Considerations on self- and parametrically excited vibrational systems. *Ing Arch* 1989;59:285–95.
- [10] Abouhazim N, Belhaq M, Lakrad F. Three-period quasi-periodic solutions in self-excited quasi-periodic Mathieu oscillator. *Nonlinear Dynam* 2005;39:395–409.
- [11] Pandey M, Rand RH, Zehnder A. Frequency locking in a forced Mathieu–van der Pol–Duffing system. *Nonlinear Dynam* 2007. doi:10.1007/s11071-007-9238-x.
- [12] Pandey M, Rand RH, Zehnder A. Perturbation analysis of entrainment in a micromechanical limit cycle oscillator. *Commun Nonlinear Sci Numer Simul* 2007;12:1291–301.
- [13] Chelomei VN. Mechanical paradoxes caused by vibrations. *Soviet Phys Dokl* 1983;28:387–90.
- [14] Tcherniak D. The influence of fast excitation on a continuous system. *J Sound Vib* 1999;227(2):343–60.
- [15] Thomsen JJ. Some general effects of strong high-frequency excitation: stiffening, biasing, and smoothening. *J Sound Vib* 2002;253(4):807–31.
- [16] Jensen JS, Tcherniak DM, Thomsen JJ. Stiffening effects of high-frequency excitation: experiments for an axially loaded beam. *J Appl Mech* 2000;67(2):397–402.
- [17] Hansen MH. Effect of high-frequency excitation on natural frequencies of spinning discs. *J Sound Vib* 2000;234(4):577–89.
- [18] Chatterjee S, Singha TK, Karmakar SK. Non-trivial effect of fast vibration on the dynamics of a class of nonlinearly damped mechanical systems. *J Sound Vib* 2003;260(4):711–30.
- [19] Thomsen JJ. Using fast vibrations to quench friction-induced oscillations. *J Sound Vib* 1999;228(5):1079–102.
- [20] Mann BP, Koplou MA. Symmetry breaking bifurcations of a parametrically excited pendulum. *Nonlinear Dynam* 2006;46:427–37.
- [21] Sah SM, Belhaq M. Effect of vertical high-frequency parametric excitation on self-excited motion in a delayed van der Pol oscillator. *Chaos Soliton Fract* 2006. doi:10.1016/j.chaos.2006.10.040.

- [22] Belhaq M, Sah SM. Horizontal fast excitation in delayed van der Pol oscillator. *Commun Nonlinear Sci Numer Simul* 2007. doi:[10.1016/j.cnsns.2007.02.007](https://doi.org/10.1016/j.cnsns.2007.02.007).
- [23] Blekhman II. *Vibrational mechanics – nonlinear dynamic effects, general approach, application*. Singapore: World Scientific; 2000.
- [24] Belhaq M, Houssni M. Quasi-periodic oscillations, chaos and suppression of chaos in a nonlinear oscillator driven by parametric and external excitations. *Nonlinear Dynam* 1999;18:1–24.
- [25] Rand RH, Guennoun K, Belhaq M. 2:2:1 Resonance in the quasi-periodic Mathieu equation. *Nonlinear Dynam* 2003;31:187–93.
- [26] Abouhazim N, Rand RH, Belhaq M. The damped nonlinear quasi-periodic Mathieu equation near 2:2:1 resonance. *Nonlinear Dynam* 2006;45:237–47.
- [27] Nayfeh AH, Mook DT. *Nonlinear oscillations*. New York: Wiley; 1979.